



Calorimetric, dilatometric and DTA under pressure studies of the phase transitions in elpasolite $(\text{NH}_4)_2\text{KZrF}_7$

Mikhail V. Gorev^{a,b}, Andrey V. Kartashev^{a,c}, Evgeniy V. Bogdanov^{a,d}, Igor N. Flerov^{a,b,*}, Natalia M. Laptash^e

^a Kirensky Institute of Physics, Federal Research Center KSC SB RAS, 660036, Krasnoyarsk, Russia

^b Institute of Engineering Physics and Radioelectronics, Siberian Federal University, 660074, Krasnoyarsk, Russia

^c Astafjev Krasnoyarsk State Pedagogical University, 660049, Krasnoyarsk, Russia

^d Institute of Engineering Systems and Energy, Krasnoyarsk State Agrarian University, 660049, Krasnoyarsk, Russia

^e Institute of Chemistry, Far Eastern Department of RAS, 690022, Vladivostok, Russia



ARTICLE INFO

Keywords:

Phase transition
Fluorides
Heat capacity
Entropy
Thermal expansion
High pressure

ABSTRACT

Heat capacity, thermal expansion, and sensitivity to the hydrostatic pressure of $(\text{NH}_4)_2\text{KZrF}_7$ elpasolite are studied in a wide temperature range. The changes in deformation and entropy during successive phase transitions are determined: $\Delta(\Delta V/V) = 3 \cdot 10^{-4}$; $\Delta S = 8 \text{ J/mol K}$. The temperatures and entropies of phase transitions turned out to be slightly sensitive to pressure changes. An analysis of the entropy of phase transformations was performed in the framework of the model of the cubic phase structure Fm-3 m. In the low temperature phase, an anomalous behavior of thermodynamic properties, which is not characteristic of phase transitions, was observed, accompanied by a significant change in the crystal lattice entropy.

1. Introduction

Numerous studies of complex fluorides and their solid solutions have shown that anionic-cationic substitution can significantly affect the formation of the type of structure, its change during phase transitions and the behavior of physical properties [1–7]. For example, the substitution of the central atom or monovalent cations in six-coordinated compounds $\text{A}_2\text{A}'\text{MF}_6$ (A, A': Cs, Rb, K, NH_4 ; M: Lu, Sc, Fe, Ga, Al) [4,6,8–13] and $(\text{NH}_4)_2\text{MF}_6 \cdot \text{NH}_4\text{F}$ (M: Si, Ge, Ti, Sn, Pb) [14–23] does not change the cubic Fm-3 m symmetry of the initial phase but leads to strong change in the succession of structural distortions associated with the nonferroelectric transformations and their parameters (degree of the structural disordering, temperature, entropy, sensitivity to external pressure, etc.).

Other situation was observed in fluorides with seven-coordinated anionic polyhedra which can be formed as a monocapped trigonal prism (A_2MF_7 ; A: Rb, NH_4 , K; M: Ta, Nb) [24–30] or a pentagonal bipyramid (A_3MF_7 ; A: K, NH_4 ; M: Hf, Zr) [31–36]. The variation of cations and central atom in the former compounds is accompanied by strong change in the symmetry and structural disorder in the initial and distorted phases. On the other hand, the latter fluorides show rather different sensitivity to cationic and anionic replacement. Thermodynamic parameters of the ammonium hafnium compound, including

the temperatures and entropies of transformations, are very close to those of the zirconium crystal [32,33]. However, the complete or even partial replacement of the tetrahedral ammonium cation with spherical potassium in A_3ZrF_7 leads to a significant decrease in the number of phase transitions and a change in their sequence [37–40].

Summarizing the above, we can conclude that chemical pressure is one of the most effective tools in the search and design of new fluorine materials. This statement is confirmed by the results of recent pioneering research of the first synthesized complex fluorine elpasolite $(\text{NH}_4)_2\text{KZrF}_7$ [40]. X-ray and optical studies have shown that its structure in the initial phase is characterized by the same cubic symmetry Fm-3 m that was determined for the initial $(\text{NH}_4)_3\text{ZrF}_7$ cryolite [32]. On the other hand, the temperature behavior of structure and optical properties has demonstrated that elpasolite undergoes only two structural transformations Fm-3 m ($T_1 = 333 \text{ K}$) \leftrightarrow P4₂/ncm ($T_2 = 329 \text{ K}$) \leftrightarrow P4₂/nmc [40] instead of six phase transitions accompanied by stronger structural distortions observed in cryolite. It cannot be ruled out that such a strong difference in the structural parameters of two related crystals is due to a small difference in the ionic radii of potassium and ammonium, which led to the occupation of nonequivalent crystallographic positions 4c and 8c by both cations that was found by the refinement of structure.

These structural features of elpasolite should certainly affect its

* Corresponding author at: Kirensky Institute of Physics, Federal Research Center KSC SB RAS, 660036, Krasnoyarsk, Russia.

E-mail address: flerov@iph.krasn.ru (I.N. Flerov).

<https://doi.org/10.1016/j.jfluchem.2020.109523>

Received 15 December 2019; Received in revised form 13 March 2020; Accepted 3 April 2020

Available online 25 April 2020

0022-1139/ © 2020 Elsevier B.V. All rights reserved.

thermodynamic properties. In this regard, it is of undoubted interest to clarify the issue related to the entropy and deformation parameters of the $(\text{NH}_4)_2\text{KZrF}_7$ crystal. In the present paper, we performed detailed investigations of the heat capacity, thermal expansion, and the sensitivity of temperatures and entropies of phase transitions to hydrostatic pressure.

2. Experimental

Samples of $(\text{NH}_4)_2\text{KZrF}_7$ were synthesized by mixing aqueous solutions $(\text{NH}_4)_3\text{ZrF}_7$, NH_4F and KHF_2 at a component ratio of 1: 1.5: 1.1. If the solution becomes cloudy, a few drops of hydrofluoric acid (40 % wt) should be added. The solution in a platinum cup was evaporated in a water bath until a crystalline film appeared. During cooling and continuous stirring of the solution, a plentiful fine crystalline precipitate was formed, which was washed with alcohol and air-dried. The composition of the crystals was controlled by the content of potassium, determined by atomic absorption.

Characterization of the sample under study was carried out in the cubic phase $Fm-3m$ at 368 K ($a = 9.2904 \text{ \AA}$) by XRD using a Bruker D8 ADVANCE powder diffractometer (Cu-K α radiation). In accordance with the results of Rietveld refinement, no additional phases were observed in $(\text{NH}_4)_2\text{KZrF}_7$ (Fig. 1).

Due to the very small size of the single crystals ($\leq 100 \mu\text{m}$), measurements of the heat capacity and thermal expansion were carried out on samples prepared as quasi-ceramic disk-shaped pellets of 4 mm diameter and 1.0–2.0 mm thickness under pressure without heat treatments because of the presence of ammonium ions. Experiments with differential thermal analysis (DTA) under high pressure were performed on powdered sample of $(\text{NH}_4)_2\text{KZrF}_7$.

Measurements of thermal expansion were performed using a push-rod dilatometer (NETZSCH model DIL-402C) with a fused silica sample holder. Experiments were carried out in the temperature range 100–370 K with a heating rate of 3 K/min in a dry He flux. In order to remove the influence of system thermal expansion, the results were calibrated by taking quartz as the standard reference. The discrepancy in the data obtained in successive series of measurements was less than 5%.

Heat capacity measurements were performed in a wide temperature range of 100–340 K by means of a home-made adiabatic calorimeter with three screens, as described in [41]. The mass of the sample was about 0.3 g. The error in determining the specific heat was less than 0.5–1.0%. The heat capacity of the “sample + heater + contact grease” system was measured using discrete as well as continuous heating. In the former case, the calorimetric step was varied from 1.5 to 3.0 K. In the latter case, the system was heated at rates of $dT/dt \approx 0.15\text{--}0.30 \text{ K/min}$. The heat capacities of the heater and contact grease were

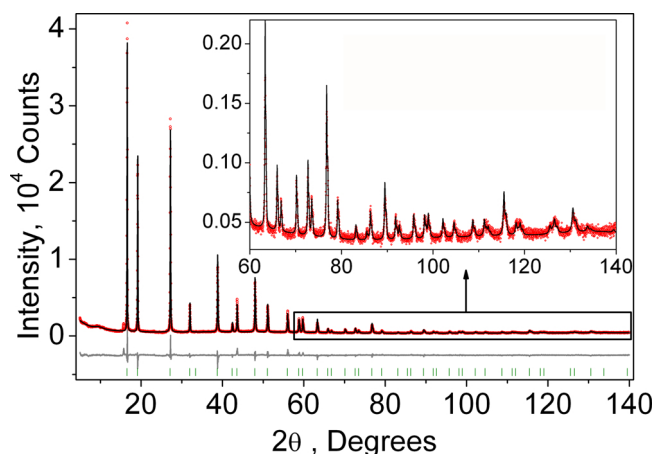


Fig. 1. Difference Rietveld plot of $(\text{NH}_4)_2\text{KZrF}_7$ ($Fm-3m$) at 368 K.

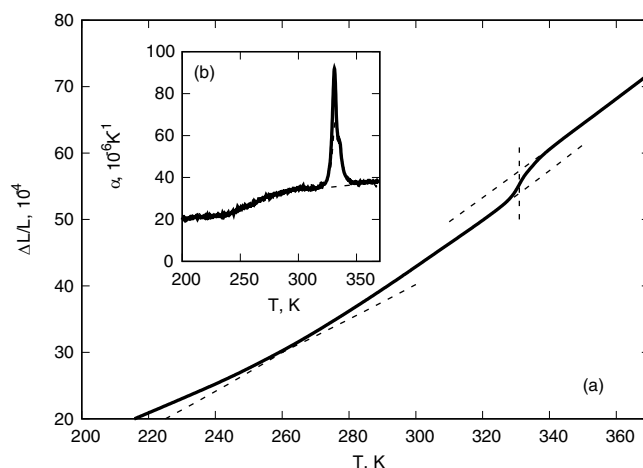


Fig. 2. Temperature dependences of (a) strain of $(\text{NH}_4)_2\text{KZrF}_7$ and (b) the thermal expansion coefficient obtained in two series of measurements. Dashed line in (a) is a lattice contribution in the region of phase transitions.

determined in individual experiments.

DTA setup was used to study the effect of hydrostatic pressure on the temperatures and enthalpy/entropy of the $Fm-3m \leftrightarrow P4_2/nmc \leftrightarrow P4_2/nmc$ phase transitions. A copper container with a powder sample of 0.05 g and the reference quartz sample were glued onto opposite junctions of a highly sensitive ($\sim 400 \mu\text{V/K}$) germanium-copper thermocouple. The system, mounted in such a manner, was placed inside a piston-cylinder type vessel which was associated with a pressure multiplier. Pressure up to 0.25 GPa was generated using silicon oil as the pressure-transmitting medium. Temperature and pressure were measured with a copper-constantan thermocouple and manganin gauge with accuracies of about $\pm 1 \text{ K}$ and $\pm 10^{-3} \text{ GPa}$, respectively.

3. Results and discussion

Fig. 2 shows the results of the thermal dilatation measurements on $(\text{NH}_4)_2\text{KZrF}_7$. It can be seen that in the temperature range of two successive phase transitions observed in [40], the behavior of linear strain, $\Delta L/L_0$, and the coefficient of linear thermal expansion, α , is anomalous at temperatures: $T_1 = 335.0 \pm 1.0 \text{ K}$, $T_2 = 331.0 \pm 0.5 \text{ K}$. Because of the slight temperature difference, $T_1 - T_2$, the values of the change in $\Delta L/L_0$ associated with each transformation can not be determined. Total positive “jump” of the linear deformation associated with both phase transitions is rather small $\sim 3 \cdot 10^{-4}$.

Additional anomalous behavior of the thermal expansion was observed below room temperature. The $\Delta L/L_0(T)$ and $\alpha(T)$ curves demonstrate a kink at about 250–260 K and step-wise increase from $20 \cdot 10^{-6}$ to $30 \cdot 10^{-6}$ in a very broad temperature range: 235–270, respectively (Fig. 2). Optical properties did not show any features at these temperatures [40]. X-ray patterns at 300 K and 150 K turned out to be the same.

As usual, the $\alpha(T)$ dependence in high temperature phase is considered as the lattice contribution α_{lat} . Extrapolation of the curve $\alpha(T)$ above T_1 to low temperature phase $P4_2/nmc$ shows a good agreement with the value of α just below T_2 down to 285 K.

As to the anomalies in the dependences $\Delta L/L_0(T)$ and $\alpha(T)$ in the tetragonal $P4_2/nmc$ phase, the absence of any features in the behavior of the optical properties and structure suggests that this phenomenon can be associated with a change in the thermal expansion of the crystal lattice. It is currently difficult to imagine the reasons for this behavior of $\Delta L/L_0$ and α . It is obvious that further studies of $(\text{NH}_4)_2\text{KZrF}_7$ are needed. For example, NMR data may turn out to be very useful since it cannot be ruled out that the discussed low-temperature anomalies may be related to a change in the mobility of ammonium groups.

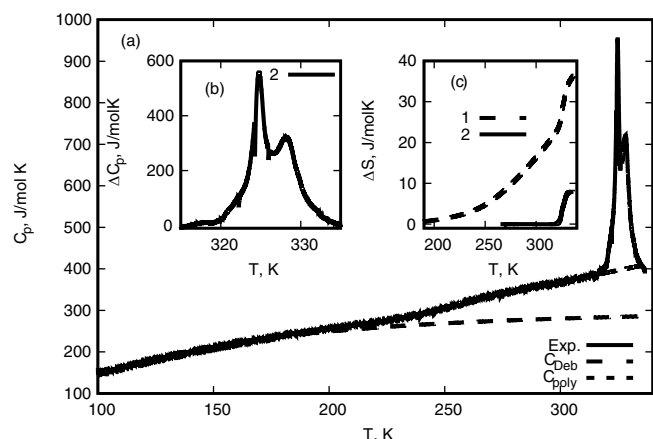


Fig. 3. Temperature dependencies of (a) heat capacity C_p , (b) anomalous heat capacity ΔC_p , and (c) anomalous entropy ΔS of $(\text{NH}_4)_2\text{KZrF}_7$. Dotted and dashed lines in (a) are heat capacities determined using the Debye model, C_{Deb} , and polynomial approximation, C_{poly} , respectively. Curves 1 and 2 are ΔC_p (b) and ΔS (c) determined in the framework of the Debye and polynomial models.

Data on the heat capacity, C_p , of $(\text{NH}_4)_2\text{KZrF}_7$ obtained as a result of experiments using an adiabatic calorimeter (AC) are shown in Fig. 3. The behavior of $C_p(T)$ turned out similar to that observed for $\alpha(T)$. Firstly, two features associated with successive phase transitions are found. Secondly, an anomalous behavior of $C_p(T)$ was observed in almost the same temperature range of the $\text{P4}_2/\text{nmc}$ phase, where a stepwise change in $\alpha(T)$ was found.

The temperatures of the heat capacity anomalies, $T_1 = 328.2 \pm 0.1$ K and $T_2 = 324.8 \pm 0.1$ K, associated with the phase transitions are lower than those determined in measurements with a differential scanning calorimeter (DSC) ($T_1 = 332.5 \pm 1.0$ K; $T_2 = 329.2 \pm 1.0$ K) [40] and dilatometer (Dil) ($T_1 = 335.0 \pm 1.0$ K, $T_2 = 331.0 \pm 0.5$ K.). However, taking into account a rather large difference in the rate of temperature change in measurements using different devices (AC: $dT/dt \approx 0.2$ K/min; DSC: 8 K/min; Dil: 3 K/min), which are equipped with thermal sensors of different sensitivity and accuracy, having different thermal contact with the sample under study, the difference in T_i can be considered insignificant.

Due to the complex behavior of the heat capacity of $(\text{NH}_4)_2\text{KZrF}_7$, it is practically impossible to follow the above methodology in the entire interval of the studied temperatures. Therefore, the separation of the

different contributions into total C_p is carried out in two ways. Firstly, the data on the heat capacity below 200 K were approximated within the framework of the Debye model and dependence $C_{\text{Deb}}(T)$ was extrapolated to the region of high temperatures. Secondly, the polynomial function was used to approximate $C_p(T)$ only in the $\text{P4}_2/\text{nmc}$ phase between 265 K and 310 K. In high temperature cubic phase, namely above 340 K, data on $C_p(T)$ are not available due to the chemical decomposition of $(\text{NH}_4)_2\text{KZrF}_7$ in high vacuum (10^{-6} mm Hg) used in measurements in the adiabatic calorimeter.

The results of using both approximations are shown in Fig. 3 as a dotted and dashed lines. Excess heat capacity associated only with successive transformations, $\Delta C_p = C_p - C_{\text{Lat}}$, reaches large values at T_1 and T_2 but exits in narrow temperature range, ~ 10 K (Fig. 3a). It is seen also that the contributions ΔC_p associated with the individual phase transitions are overlapped. That is why it was possible to determine only the value of the total change in excess entropy as the sum $\Sigma \Delta S_i = \Delta S_1 + \Delta S_2 = \int (\Delta C_p/T) dT = 8 \pm 1$ J/mol K. This value is rather large and close to $R \ln 3$ which allows us to assume that structural distortions in elpasolite $(\text{NH}_4)_2\text{KZrF}_7$ may be related to order-disorder processes during the phase transitions.

Fig. 3c shows the behavior of excess entropy $\Sigma \Delta S_i$ as well as the difference between total entropy and entropy associated with the contribution of the Debye heat capacity $\Delta S_{\text{Deb}}(T) = S(T) - S_{\text{Deb}}$, where $S(T) = \int (C_p/T) dT$ and $S_{\text{Deb}}(T) = \int (C_{\text{Deb}}/T) dT$. The large difference between the values of ΔS_{Deb} and $\Sigma \Delta S_i$ can also be considered as related to the possible change in the mobility of structural elements that was suggested above.

The results of a study of the sensitivity of elpasolite to hydrostatic pressure are presented in Fig. 4a. It can be seen that in the region of phase transitions, two anomalies of the DTA signal are reliably recorded both at atmospheric and high pressure. However, the sensitivity of the DTA method was not enough to record an abnormal behavior in the tetragonal $\text{P4}_2/\text{nmc}$ phase, where a stepwise increase in both $\alpha(T)$ and $C_p(T)$ was observed.

The pressure increase does not cause a significant change in the values of the anomalous DTA signal, the temperatures of the signal maxima, as well as the area under the anomalies, which corresponds to the enthalpy/entropy of phase transitions. The latter result suggests that the constancy of excess entropy under pressure is apparently a common feature characteristic of fluorides and oxyfluorides. Indeed, the same situation was observed by us earlier in the study of elpasolites Rb_2KFeF_6 , RbKTiOF_5 [42,43] and cryolites $(\text{NH}_4)_3\text{TiOF}_5$, $(\text{NH}_4)_3\text{NbOF}_6$ [44], etc.

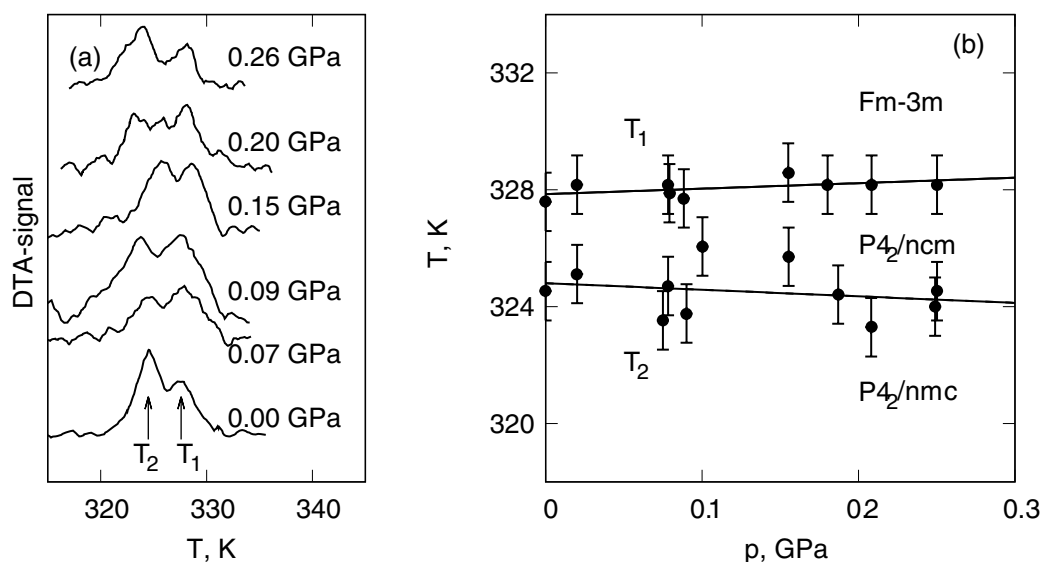


Fig. 4. (a) Temperature dependencies of DTA-signal at different pressures and (b) temperature-pressure phase diagram of $(\text{NH}_4)_2\text{KZrF}_7$.

A positive sign of both anomalies on the dependence $\alpha(T)$ (Fig. 2) means that the temperatures of both phase transitions should increase under pressure. The experimentally investigated T-p phase diagram shown in Fig. 4b agrees well with this assumption. The baric coefficients were determined with a large error, $dT_1/dp = +1.9 \pm 1.1$ K/GPa and $dT_2/dp = -2.2 \pm 3.2$ K/GPa, for several reasons. First, this is due to the very weak pressure dependence of the T_1 and T_2 temperatures. Secondly, the temperature sensor in the DTA installation has a fairly low accuracy. A rather significant smearing of the anomalous part of the DTA-signal, which leads to difficulties in accurately determining T_1 and T_2 , is the third reason.

Due to the overlap of the anomalous contributions to thermal expansion and heat capacity (Fig. 2 and 3), it is impossible to accurately determine the magnitudes of the deformation, $\delta(\Delta L/L)$, and entropy, $\delta S \approx \Delta S$, jumps and then calculate the baric coefficients using the Clapeyron-Clausius equation, $dT/dp = \delta(\Delta V/V)/\delta S$, where $\delta(\Delta V/V) = 3\delta(\Delta L/L)$. However, the behavior of $\alpha(T)$ and $C_p(T)$ in the region of phase transitions (Figs. 2a and 3 a) allows us to assume that the changes in deformation and entropy at T_1 and T_2 are the same for both transformations: $\delta(\Delta V/V) \approx (3.5 \pm 1.0) \cdot 10^{-4}$, $\delta S = (4.0 \pm 1.0)$ J/mol·K. Of course, this approximation leads to a large error in determining individual values of anomalous entropy and deformation. Nevertheless, despite large errors, it is obvious that the calculated values of the temperature shift of the phase transitions under pressure, $dT_i/dp = (10 \pm 5)$ K/GPa, are of the same order as the baric coefficients determined experimentally.

On the one hand, the substitution of tetrahedral ammonium cation in crystallographic site 4b by spherical potassium in cryolite $(NH_4)_3ZrF_7$ did not affect the symmetry of the initial cubic phase, (Fm-3 m), but on the other hand, leads to strong change in the number of the phase transitions and the symmetry of distorted phases in elpasolite $(NH_4)_2KZrF_7$ [40]. As it was mentioned above, due to the large unit cell volume, numerous refinement parameters and the disordering of the ZrF_7 polyhedron, the crystal structure of elpasolite was not solved in experiments using X-ray powder diffractometer [40]. Nevertheless, we can consider the data on the thermodynamic properties of elpasolite in comparison with those for cryolite $(NH_4)_3ZrF_7$ [32] taking into account the data on its structure as well as related $(NH_4)_3HfF_7$ in the cubic phase [35,36].

Recently, the cryolite cubic structure of some ammonium fluorides and oxyfluorides, including $(NH_4)_3ZrF_7$, was revised X-ray single crystal diffractometer and structural model was suggested for disordered initial cubic Fm-3 m phase [36]. A pentagonal bipyramid ZrF_7 with $mm2$ local symmetry was considered as a rigid body which should be orientationally disordered at least on 12 equal positions to preserve a cubic symmetry of crystal lattice. Ammonium groups were also assumed to be disordered having four (8c site) and eight (4b site) spatial orientation. Despite the lack of a refinement of the structure for $(NH_4)_2KZrF_7$, it is highly likely that in the ideal elpasolite structure two ammonium ions in position 8c are also disordered while the spherical potassium cation in position 4b is ordered.

Using models of both disordered structures, one can evaluate the possible entropies change in the case of the total ordering of structural elements. This value is equal to $\Delta S_{total} = R(\ln 12 + 2\ln 4 + \ln 8) \approx 61$ J/mol K for cryolite and $\Delta S_{total} = R(\ln 12 + 2\ln 4) \approx 44$ J/mol K for elpasolites. Both values are significantly excess the entropies determined experimentally: $(\Sigma \Delta S_i)_{exp} = 14.5$ J/molK $\approx R \ln 6$ [32] and $(\Sigma \Delta S_i)_{exp} = 8$ J/mol K $\approx R \ln 3$ for $(NH_4)_3ZrF_7$ and $(NH_4)_2KZrF_7$, respectively.

It is necessary to pay attention to the interesting feature of the elpasolite structure revealed during X-ray studies [40]. Both non-equivalent crystallographic positions, 8c and 4b, were occupied by NH_4/K mixed ions with refined occupancies and linear restriction $occ(NH_4) + occ(K) = 1$ for all sites. Real chemical formula was suggested as $[(NH_4)_{0.672}K_{0.328}]_2[(NH_4)_{0.732}K_{0.268}]ZrF_7$. Thus, crystallographic positions inside the octahedron, 4b, and in the interoctahedral cavity, 8c, are occupied by both potassium atoms and ammonium groups. In this

case the total ordering of the disordered Fm-3 m structure leads to increase in the entropy change in comparison with $(NH_4)_2KZrF_7$ $\Delta S_{total} = R(\ln 12 + 1.35 \ln 4 + 0.732 \ln 8) = 49$ J/mol K.

The comparison of the calculated and experimentally determined entropies of phase transitions in both cryolite and elpasolite is not entirely correct, since the calculation was carried out for the case of complete ordering of structural elements disordered in the cubic phase. It is obvious that more accurate calculations can be performed only after careful studies of the structure of distorted phases, which will allow us to establish a real change in the degree of disordering of structural elements during phase transitions. Nevertheless, at this stage, we can consider several possible circumstances that are the cause of the revealed significant difference in the values of ΔS_{total} and $(\Sigma \Delta S_i)_{exp}$.

Firstly, some structural elements can remain disordered in distorted phases, which can lead to additional phase transitions in both investigated fluorides in the temperature range below the lowest temperature used in the experiments. However, at least for cryolite, the Raman study did not reveal any peculiarities in the spectra below $T_4 = 240$ K down to 7 K [45].

Secondly, some disorder persists up to 0 K, which leads to residual entropy. To verify this hypothesis, calorimetric studies at very low temperatures are required.

Thirdly, there is no such strong disordering of the structure in phase Fm-3 m that was proposed in the model [36] and the cubic symmetry is preserved due to the strong anharmonicity of vibrations of critical structural elements without their fixation in certain crystallographic positions. In this case, the entropy of phase transitions has some intermediate values that are proportional to the degree of anharmonicity and can significantly exceed the entropies characteristic of displacive-type transitions, remaining much smaller than the entropies associated with the order-disorder processes. This assumption is supported by the results of studies of the Raman spectra of cryolite, which were interpreted as associated with slowing of the ammonium ion's motion along with the temperature decrease, but not with their ordering [45]. Moreover, the localized positions on electron density maps corresponding to disordering are not visible for some critical elements [35].

Thus, it can be assumed that the models of the cubic phase in complex fluorides are associated with the maximum possible disordering of structure [10,35,36].

Due to different successions of structural distortions, a joint detailed analysis of the T-p phase diagrams of elpasolite and cryolite is impossible. However, despite the fact that pressure suppresses the anomaly at T_0 , one can evaluate the effect of cationic substitution $K^+ \rightarrow NH_4^+$ on the stability of the cubic phase under pressure in cryolite. Using the data of $C_p(T)$ and $\alpha(T)$ for $(NH_4)_3ZrF_7$ [32], we made rough estimates of the sensitivity of the second-order phase transition from the cubic phase in the framework of the Ehrenfest equation: $dT_0/dp \approx +10$ K/GPa. This value is not much larger than the experimentally found in the present work for elpasolite: $dT_1/dp \approx +2$ K/GPa.

As for the anomalous stepwise behavior of $C_p(T)$ and $\alpha(T)$ in the low-temperature phase of the elpasolite $(NH_4)_2KZrF_7$, it should be noted that this unusual phenomenon is observed in the temperature region where the cryolite $(NH_4)_3ZrF_7$ undergoes three low-temperature phase transitions [32].

At the same temperatures, very complex twinning was observed and the strong influence of thermal cycling on the properties of the crystal, especially on thermal expansion.

4. Conclusions

Calorimetric, dilatometric and DTA under hydrostatic pressure studies were performed on elpasolite $(NH_4)_2KZrF_7$ in a wide temperature range including phase transitions $Fm-3 m \rightarrow P4_2/ncm \rightarrow P4_2/nmc$ [40].

Heat capacity and thermal expansion exhibit anomalous behavior in both structural transformations. However, the overlap of the anomalous

contributions to linear strain, $\Delta L/L(T)$, and heat capacity, $C_p(T)$, prevents the exact determination of the changes in deformation and entropy during phase transformations. The magnitudes of the complete change in both thermodynamic parameters are as follows: $\Delta(\Delta V/V) \approx 3 \cdot 10^{-4}$, $\Delta S \approx 8 \text{ J/mol K}$.

Very small values of baric coefficients, $dT_1 / dp \approx +1.9 \pm 1.1 \text{ K/GPa}$ and $dT_2 / dp \approx -2.2 \pm 3.2 \text{ K/GPa}$, determined in direct measurements, indicate a low sensitivity of elpasolite to external pressure. Entropy of phase transitions was also very stable with respect to hydrostatic pressure, as was observed for other related complex fluorides [42–44].

A joint analysis of structural and calorimetric data was performed for some fluoride elpasolites-cryolites, including $(\text{NH}_4)_2\text{KZrF}_7$ and $(\text{NH}_4)_3\text{ZrF}_7$. It was suggested that the proposed structural models [10,35,36] are associated with the maximum possible disordering of critical elements.

The anomalous behavior of the studied thermodynamic properties of $(\text{NH}_4)_2\text{KZrF}_7$, which is not characteristic of phase transitions, was found in the tetragonal phase $P4_2/nmc$ in the temperature range where the $(\text{NH}_4)_3\text{ZrF}_7$ cryolite undergoes three phase transitions [32]. To clarify the nature of the detected phenomenon, accompanied by a very large change in entropy, at least studies of the NMR spectra will be useful.

Declaration of Competing Interest

The authors declare that they have no known competing financial interests or personal relationships that could have appeared to influence the work reported in this paper

Acknowledgements

The reported study was funded by RFBR according to the research project No. 18-02-00269 a. X-ray and dilatometric data were obtained using the equipment of Krasnoyarsk Regional Center of Research Equipment of Federal Research Center "Krasnoyarsk Science Center SB RAS".

References

- [1] A. Tressaud (Ed.), *Functionalized Inorganic Fluorides: Synthesis, Characterization and Properties of Nanostructured Solids*, Wiley-Blackwell, 2010, <https://doi.org/10.1002/9780470660768>.
- [2] M. Leblanc, V. Maisonneuve, A. Tressaud, Crystal chemistry and selected physical properties of inorganic fluorides and oxide-fluorides, *Chem. Rev.* 115 (2015) 1191–1254, <https://doi.org/10.1021/cr500173c>.
- [3] Z. Mazej, R. Hagiwara, Hexafluoro-, heptafluoro-, and octafluoro-salts, and $[\text{M}_n\text{F}_{5n+1}]^-$ ($n = 2, 3, 4$) polyfluorometallates of singly charged metal cations, Li^+ - Cs^+ , Cu^+ , Ag^+ , In^+ and Tl^+ , *J. Fluorine Chem.* 128 (2007) 423–437, <https://doi.org/10.1016/j.jfluchem.2006.10.007>.
- [4] I. Flerov, M. Gorev, M. Molokeev, N. Laptash, Ferroelastic and ferroelectric phase transitions in fluoro- and oxyfluorometallates, in: A. Tressaud, K. Poeppelmeier (Eds.), *Photonic and Electronic Properties of Fluoride Materials*, Elsevier, Boston, 2016, pp. 355–381, <https://doi.org/10.1016/B978-0-12-801639-8.00016-7>.
- [5] T. Nakajima, B. Zemva, A. Tressaud, *Advanced Inorganic Fluorides: Synthesis, Characterization and Applications*, Elsevier Science, Amsterdam, 2000.
- [6] C.-F. Mu, Q.-Z. Yao, G.-T. Zhou, S.-Q. Fu, Three-dimensional architectures of $(\text{NH}_4)_3\text{AlF}_6$ solid solution: synthesis, shape evolution, and growth mechanism, *Cryst. Growth Des.* 10 (2010) 3869–3878, <https://doi.org/10.1021/cg100016f>.
- [7] J.F. Scott, R. Blinc, Multiferroic magnetoelectric fluorides: why are there so many magnetic ferroelectrics? *J. Phys. Condens. Matter* 23 (2011) 113202, <https://doi.org/10.1088/0953-8984/23/11/113202>.
- [8] M.V. Gorev, I.N. Flerov, A. Tressaud, Thermodynamic properties and p-T phase diagrams of $(\text{NH}_4)_3\text{M}^{3+}\text{F}_6$ cryolites (M^{3+} : Ga, Sc), *J. Phys. Condens. Matter* 11 (1999) 7493–7500, <https://doi.org/10.1088/0953-8984/11/39/306>.
- [9] I. Flerov, M. Gorev, J. Granec, A. Tressaud, Role of metal fluoride octahedra in the mechanism of phase transitions in A_2BMF_6 elpasolites, *J. Fluorine Chem.* 116 (2002) 9–14, [https://doi.org/10.1016/S0022-1139\(02\)00068-4](https://doi.org/10.1016/S0022-1139(02)00068-4).
- [10] A.A. Udovenko, N.M. Laptash, I.G. Maslennikova, Orientation disorder in ammonium elpasolites. Crystal structures of $(\text{NH}_4)_3\text{AlF}_6$, $(\text{NH}_4)_3\text{TiOF}_5$ and $(\text{NH}_4)_3\text{FeF}_6$, *J. Fluorine Chem.* 124 (2003) 5–15, [https://doi.org/10.1016/S0022-1139\(03\)00166-0](https://doi.org/10.1016/S0022-1139(03)00166-0).
- [11] I.N. Flerov, M.V. Gorev, K.S. Aleksandrov, A. Tressaud, V.D. Fokina, Ferroelastic phase transitions in fluorides with cryolite and elpasolite structures, *Crystallogr. Rep.* 49 (2004) 100–107, <https://doi.org/10.1134/1.1643969>.
- [12] J. Lin, S.-M. Luo, H.-Y. Sun, X.-X. Liu, Z.-B. Wie, Syntheses and characterization of elpasolite-type ammonium alkali metal hexafluorometallates(III), *J. Solid State Chem.* 181 (2008) 1723–1730, <https://doi.org/10.1016/j.jssc.2008.03.017>.
- [13] M. Gorev, E. Bogdanov, I. Flerov, T-p phase diagrams and the barocaloric effect in materials with successive phase transitions, *J. Phys. D Appl. Phys.* 50 (2017) 384002, <https://doi.org/10.1088/1361-6463/aa8025>.
- [14] U. Reusch, E. Schweda, In situ X-ray powder diffraction: the reactions of Pb(IV)-fluoride with ammonia and NH_4F , *European Powder Diffraction EPDIC 7*, Vol. 378 of Materials Science Forum, Trans Tech Publications Ltd, 2001, pp. 326–330, <https://doi.org/10.4028/www.scientific.net/MSF>.
- [15] I.M. Shlyapnikov, H.P.A. Mercier, E.A. Goresnik, G.J. Schrobilgen, Z. Mazej, Crystal structures and Raman spectra of imidazolium poly[perfluorotitanate(IV)] salts containing the $[\text{TiF}_6]^{2-}$, $(\text{Ti}_2\text{F}_9)^-$, and $[\text{Ti}_2\text{F}_{11}]^{3-}$ and the new $[\text{Ti}_4\text{F}_{20}]^{4-}$ and $[\text{Ti}_5\text{F}_{23}]^{5-}$ anions, *Inorg. Chem.* 52 (2013) 8315–8326, <https://doi.org/10.1021/ic302468j>.
- [16] M. Molokeev, S.V. Misjul, I.N. Flerov, N.M. Laptash, Reconstructive phase transition in $(\text{NH}_4)_3\text{TiF}_7$ accompanied by the ordering of TiF_6 octahedra, *Acta Cryst. B Struct. Sci.* 70 (2014) 924–931, <https://doi.org/10.1107/S2052520614021192>.
- [17] S. Mel'nikova, E. Pogoreltsev, I. Flerov, N. Laptash, Unusual sequence of phase transitions in $(\text{NH}_4)_3\text{TiF}_7$ detected by optic and calorimetric studies, *J. Fluorine Chem.* 165 (2014) 14–19, <https://doi.org/10.1016/j.jfluchem.2014.05.016>.
- [18] E. Pogoreltsev, I. Flerov, A. Kartashev, E. Bogdanov, N. Laptash, Heat capacity, entropy, dielectric properties and tp phase diagram of $(\text{NH}_4)_3\text{TiF}_7$, *J. Fluorine Chem.* 168 (2014) 247–250, <https://doi.org/10.1016/j.jfluchem.2014.10.016>.
- [19] I. Flerov, M. Molokeev, N. Laptash, A. Udovenko, E. Pogoreltsev, S. Mel'nikova, S. Misyul, Structural transformation between two cubic phases of $(\text{NH}_4)_3\text{SnF}_7$, *J. Fluorine Chem.* 178 (2015) 86–92, <https://doi.org/10.1016/j.jfluchem.2015.06.024>.
- [20] A. Kartashev, M. Gorev, E. Bogdanov, I. Flerov, N. Laptash, Thermal properties and phase transition in the fluoride, $(\text{NH}_4)_3\text{SnF}_7$, *J. Solid State Chem.* 237 (2016) 269–273, <https://doi.org/10.1016/j.jssc.2016.02.027>.
- [21] S.V. Mel'nikova, M.S. Molokeev, N.M. Laptash, S.V. Misyul, A non-typical sequence of phase transitions in $(\text{NH}_4)_3\text{GeF}_7$: optical and structural characterization, *Dalton Trans.* 45 (2016) 5321–5327, <https://doi.org/10.1039/C5DT04907E>.
- [22] E. Bogdanov, A. Kartashev, E. Pogoreltsev, M. Gorev, N. Laptash, I. Flerov, Anomalous behaviour of thermodynamic properties at successive phase transitions in $(\text{NH}_4)_3\text{GeF}_7$, *J. Solid State Chem.* 256 (2017) 162–167, <https://doi.org/10.1016/j.jssc.2017.09.010>.
- [23] S.V. Mel'nikova, M.S. Molokeev, N.M. Laptash, E.I. Pogoreltsev, S.V. Misyul, I.N. Flerov, Sequence of phase transitions in $(\text{NH}_4)_3\text{SiF}_7$, *Dalton Trans.* 46 (2017) 2609–2617, <https://doi.org/10.1039/C6DT04874A>.
- [24] V. Langer, L. Smrčok, M. Boča, Dipotassium heptafluorotantalate(V), β - K_2TaF_7 , at 509 K, *Acta Cryst. E* 62 (2006) i91–i93, <https://doi.org/10.1107/S1600536806009147>.
- [25] C. Torardi, L. Brixner, G. Blasse, Structure and luminescence of K_2TaF_7 and K_2NbF_7 , *J. Solid State Chem.* 67 (1987) 21–25, [https://doi.org/10.1016/0022-4596\(87\)90333-1](https://doi.org/10.1016/0022-4596(87)90333-1).
- [26] N. Laptash, A. Udovenko, T. Emelina, Dynamic orientation disorder in rubidium fluorotantalate. Synchronous Ta-O and Ta-F vibrations, *J. Fluorine Chem.* 132 (2011) 1152–1158, <https://doi.org/10.1016/j.jfluchem.2011.07.023>.
- [27] E. Pogoreltsev, S. Mel'nikova, A. Kartashev, M. Molokeev, M. Gorev, I. Flerov, N. Laptash, Ferroelastic phase transitions in $(\text{NH}_4)_2\text{TaF}_7$, *Phys. Solid State* 55 (2013) 611–618, <https://doi.org/10.1134/S1063783413030232>.
- [28] E.I. Pogoreltsev, S.V. Mel'nikova, A.V. Kartashev, M.V. Gorev, I.N. Flerov, N.M. Laptash, Thermal, optical, and dielectric properties of fluoride Rb_2TaF_7 , *Phys. Solid State* 59 (2017) 986–991, <https://doi.org/10.1134/S1063783417050250>.
- [29] M. Boča, A. Rakhmatullina, J. Mlynáriková, E. Hadzimoza, Z. Vaskovaa, M. Miušič, Differences in XPS and solid state NMR spectral data and thermo-chemical properties of iso-structural compounds in the series KTaF_6 , K_2TaF_7 and K_3TaF_8 and KNbF_6 , K_2NbF_7 and K_3NbF_8 , *Dalton Trans.* 44 (2015) 17106–17117, <https://doi.org/10.1039/C5DT02560E>.
- [30] L.-S. Du, R.W. Schurko, K.H. Lim, C.P. Grey, A solid-state ^{93}Nb and ^{19}F NMR spectroscopy and X-ray diffraction study of potassium heptafluoroniobate(V): characterization of ^{93}Nb , ^{19}F coupling, and fluorine motion, *J. Phys. Chem. A* 105 (2001) 760–768, <https://doi.org/10.1021/jp0032006>.
- [31] G.C. Hampson, L. Pauling, The structure of ammonium heptafluorozirconate and potassium heptafluorozirconate and the configuration of the heptafluorozirconate group, *J. Am. Chem. Soc.* 60 (1938) 2702–2707.
- [32] V. Fokina, M. Gorev, E. Bogdanov, E. Pogoreltsev, I. Flerov, N. Laptash, Thermal properties and phase transitions in $(\text{NH}_4)_3\text{ZrF}_7$, *J. Fluorine Chem.* 154 (2013) 1–6 <https://doi.org/10.1016/j.jfluchem.2013.07.001>.
- [33] E. Pogoreltsev, E. Bogdanov, S. Melnikova, I. Flerov, N. Laptash, $(\text{NH}_4)_3\text{HfF}_7$: crystalloptical and calorimetric studies of a number of successive phase transitions, *J. Fluorine Chem.* 204 (2017) 45–49, <https://doi.org/10.1016/j.jfluchem.2017.10.004>.
- [34] A. Rakhmatullina, M. Boča, J. Mlynáriková, E. Hadzimoza, Z. Vasková, I.B. Polovov, M. Mičušík, Solid state NMR and XPS of ternary fluoride-zirconates of various coordination modes, *J. Fluorine Chem.* 208 (2018) 24–35, <https://doi.org/10.1016/j.jfluchem.2018.01.010>.
- [35] A.A. Udovenko, N.M. Laptash, Orientational disorder in crystal structures of $(\text{NH}_4)_3\text{ZrF}_7$ and $(\text{NH}_4)_3\text{NbOF}_6$, *J. Struct. Chem.* 49 (2008) 482–488, <https://doi.org/10.1007/s10947-008-0066-8>.
- [36] A.A. Udovenko, A.A. Karabtsov, N.M. Laptash, Crystallographic features of ammonium fluoroelpasolites: dynamic orientational disorder in crystals of $(\text{NH}_4)_3\text{HfF}_7$

- and $(\text{NH}_4)_3\text{Ti}(\text{O}_2)\text{F}_5$, Acta Cryst. B 73 (2017) 1–9, <https://doi.org/10.1107/S2052520616017534>.
- [37] E.C. Reynhardt, J.C. Pratt, A. Watton, H.E. Petch, NMR study of molecular motion and disorder in K_3ZrF_7 and K_2TaF_7 , J. Phys. C: Solid State Phys. 14 (1981) 4701–4715, <https://doi.org/10.1088/0022-3719/14/31/017>.
- [38] M.T. Dova, M.C. Caracoché, A.M. Rodri'guez, J.A. Martínez, P.C. Rivas, A.R. Lopez Garcia, H.R. Viturro, Time-differential perturbed-angular-correlation study of phase transitions and molecular motions in $\text{K}_3(\text{Hf,Zr})\text{F}_7$, Phys. Rev. B 40 (1989) 11258–11263, <https://doi.org/10.1103/PhysRevB.40.11258>.
- [39] Yu.A. Buslaev, V.I. Pakhomov, V.P. Tarasov, V.N. Zege, F^{19} spin–lattice relaxation and X-ray study of phase transition in Solid K_3ZrF_7 and $(\text{NH}_4)_2\text{ZrF}_7$, Phys. Status Solidi (b) 44 (1971) K13–K15, <https://doi.org/10.1002/psb.2220440150>.
- [40] E.I. Pogoreltsev, S.V. Mel'nikova, M.S. Molokeev, I.N. Flerov, N.M. Laptash, Structure, thermal and optical properties of elpasolite-like $(\text{NH}_4)_2\text{KZrF}_7$, J. Solid State Chem. 277 (2019) 376–380, <https://doi.org/10.1016/j.jssc.2019.06.013>.
- [41] A.V. Kartashev, I.N. Flerov, N.V. Volkov, K.A. Sablina, Adiabatic calorimetric study of the intense magnetocaloric effect and the heat capacity of $(\text{La}_{0.4}\text{Eu}_{0.6})_{0.7}\text{Pb}_{0.3}\text{MnO}_3$, Phys. Solid State 50 (2008) 2115–2120, <https://doi.org/10.1134/S1063783408110188>.
- [42] I.N. Flerov, M.V. Gorev, A. Tressaud, N.M. Laptash, Perovskite-like fluorides and oxyfluorides: phase transitions and caloric effects, Cryst. Rep. 56 (2011) 9–17, <https://doi.org/10.1134/S106377451101010X>.
- [43] V.D. Fokina, I.N. Flerov, M.S. Molokeev, E.I. Pogorel'rtsev, E.V. Bogdanov, A.S. Krylov, A.F. Bovina, V.N. Voronov, N.M. Laptash, Heat capacity, p-T phase diagram, and structure of $\text{Rb}_2\text{KTiOF}_5$, Phys. Solid State 50 (2008) 2175–2183, <https://doi.org/10.1134/S1063783408110280>.
- [44] M. Gorev, E. Bogdanov, I. Flerov, Conventional and inverse barocaloric effects around triple points in ferroelastics $(\text{NH}_4)_3\text{NbOF}_6$ and $(\text{NH}_4)_3\text{TiOF}_5$, Scripta Mater. 139 (2017) 53–57, <https://doi.org/10.1016/j.scriptamat.2017.06.022>.
- [45] A. Krylov, S. Krylov, N. Laptash, A. Vtyurin, Raman scattering study of temperature induced phase transitions in crystalline ammonium heptafluorozirconate, $(\text{NH}_4)_3\text{ZrF}_7$, Vibrat. Spect. 62 (2012) 258–263, <https://doi.org/10.1016/j.vibspec.2012.07.003>.